

## Secondary structure of neutrophil-activating peptide-2 determined by $^1\text{H}$ -nuclear magnetic resonance spectroscopy

Kevin H. MAYO,\*† Yingqing YANG,\* Thomas J. DALY,† Jennifer K. BARRY† and Gregory J. LA ROSA†

\*Department of Biochemistry, Biomedical Engineering Center, University of Minnesota, 420 Delaware Street, S.E., Minneapolis, MN 55455, U.S.A. and †Repligen Corporation, One Kendall Square, Building 700, Cambridge, MA 02139, U.S.A.

Neutrophil-activating protein-2 (NAP-2) is a 72 residue protein demonstrating a range of proinflammatory activities. The solution structure of monomeric NAP-2 has been investigated by two-dimensional  $^1\text{H}$ -n.m.r. spectroscopy. Sequence-specific proton resonance assignments have been made and secondary structural elements have been identified on the basis of nuclear Overhauser data, coupling constants and amide hydrogen/

deuteron exchange. The NAP-2 monomer consists of a triple-stranded anti-parallel  $\beta$ -sheet arranged in a 'Greek key' and a C-terminal helix (residues 59–70) and is very similar to that found in the n.m.r. solution conformation of dimeric interleukin-8 and the crystal structure of tetrameric bovine platelet factor-4. Results are discussed in terms of heparin binding and neutrophil-activation properties of NAP-2.

### INTRODUCTION

Neutrophil-activating protein-2 (NAP-2) (Walz et al., 1989), low-affinity platelet factor 4 (LA-PF4) (Holt et al., 1986) [also named connective-tissue-activating protein III (CTAP-III) (Castor et al., 1983)], and  $\beta$ -thromboglobulin ( $\beta\text{TG}$ ) (Begg et al., 1978) are platelet-specific, naturally occurring N-terminal cleavage products of platelet basic protein (PBP) (Holt et al., 1986). All are homologues of platelet factor-4 (PF4) (Deuel et al., 1977) and are members of the growing family of C-X-C intercrines [see review by Miller and Krangel (1992)] which include interleukin-8 (IL-8) (Schmid and Weissmann, 1987; Walz et al., 1989) and Gro- $\alpha$  (Anisowicz et al., 1987). Collectively, this protein family appears to be involved in inflammation and wound healing.

NAP-2 is exceptionally potent at neutrophil activation. At nanomolar concentrations, NAP-2 induces cytosolic free calcium changes, chemotaxis with respect to neutrophils and exocytosis, while its homologues (PBP, CTAP-III and  $\beta\text{TG}$ ) are practically inactive at concentrations of less than 100–1000 nM (Walz et al., 1989). NAP-2, although less potent than IL-8, acts like IL-8 in neutrophil chemotaxis (Schnitzel et al., 1991) and competes with IL-8 for binding to neutrophil cell-surface IL-8 receptors and subsequent G-protein activation (Moser et al., 1991; Schumacher et al., 1992). Since NAP-2 devoid of its C-terminal segment is at least partially biologically active, the NAP-2 N-terminal domain which includes the N-terminus and topologically related residues, apparently possesses the neutrophil-activation properties (Holt et al., 1992).

Given the 40–60% sequence identity among proteins in the NAP-2 C-X-C family, overall structural folding is probably conserved. This has been borne out with structural studies on bovine (St. Charles et al., 1989) and human (Zhang et al., 1994) tetrameric PF4 and on dimeric human IL-8 (Clare et al., 1989), all of which fold with a C-terminal  $\alpha$ -helix stacked on to an anti-parallel  $\beta$ -sheet. Significant structural differences between PF4 and IL-8, however, can be noted in loop/turn, N-terminal and even within the C-terminal helix domain. For NAP-2, which has the same double pair of putative heparin-binding C-terminal

lysines as PF4 does, knowledge of differences/similarities, for example, within the proposed NAP-2 C-terminal helix would help to understand differences in heparin-binding properties between PF4 and NAP-2. For this reason and to aid in the identification of the neutrophil-activation site, the present study was designed to derive the solution structure of NAP-2 by using n.m.r. spectroscopy. Furthermore, in contrast with known conformations of tetrameric PF4 and dimeric IL-8, these n.m.r. structural studies have been done on monomeric NAP-2 which has been proposed to be the biologically active state (Mayo, 1991). Recently, it was shown that monomer IL-8 also constitutes that protein's functionally active state (Rajarathnam et al., 1994).

### METHODS AND MATERIALS

#### Isolation of recombinant NAP-2

The synthetic gene for human NAP-2 was expressed as a non-fusion protein in *Escherichia coli* (BL21) cells and grown at the 10 litre scale. NAP-2 was purified, cleaved and refolded essentially as previously described (Myers et al., 1991). Purity was assessed by Coomassie Blue staining of SDS/PAGE, analytical C4 reverse-phase h.p.l.c., and amino acid analysis. Typically, several hundred milligrams of more than 95% pure material was isolated from 100 g of starting material.

#### Determination of protein concentration

Protein concentrations were determined using the bicinchoninic acid (BCA) assay (Smith et al., 1985) and calculated on the basis of protein concentrations obtained from a standard dilution series of BSA. Amino acid analysis of these chemokines was obtained following hydrolysis of the proteins for 24 h at 90 °C in 12 M HCl. Samples then were derivatized and analysed according to the method of Bidlingmeyer et al. (1984). Protein concentrations were checked also by the methods of Lowry et al. (1951) and of Waddell (1956).

Abbreviations used: PBP, platelet basic protein;  $\beta\text{TG}$ ,  $\beta$ -thromboglobulin; NAP-2, neutrophil-activating peptide-2; CTAP-III, connective-tissue-activating protein-III; PF4, platelet factor 4; LA-PF4, low-affinity PF4; IL-8, interleukin-8; nOesy, two-dimensional-n.m.r. nuclear Overhauser effect spectroscopy; nOe, nuclear Overhauser effect; FID, free induction decay; DG, distance geometry; BCA, bicinchoninic acid; COSY, correlated spectroscopy; HOHAHA, homonuclear Hartmann-Hahn magnetization transfer.

† To whom correspondence should be addressed.

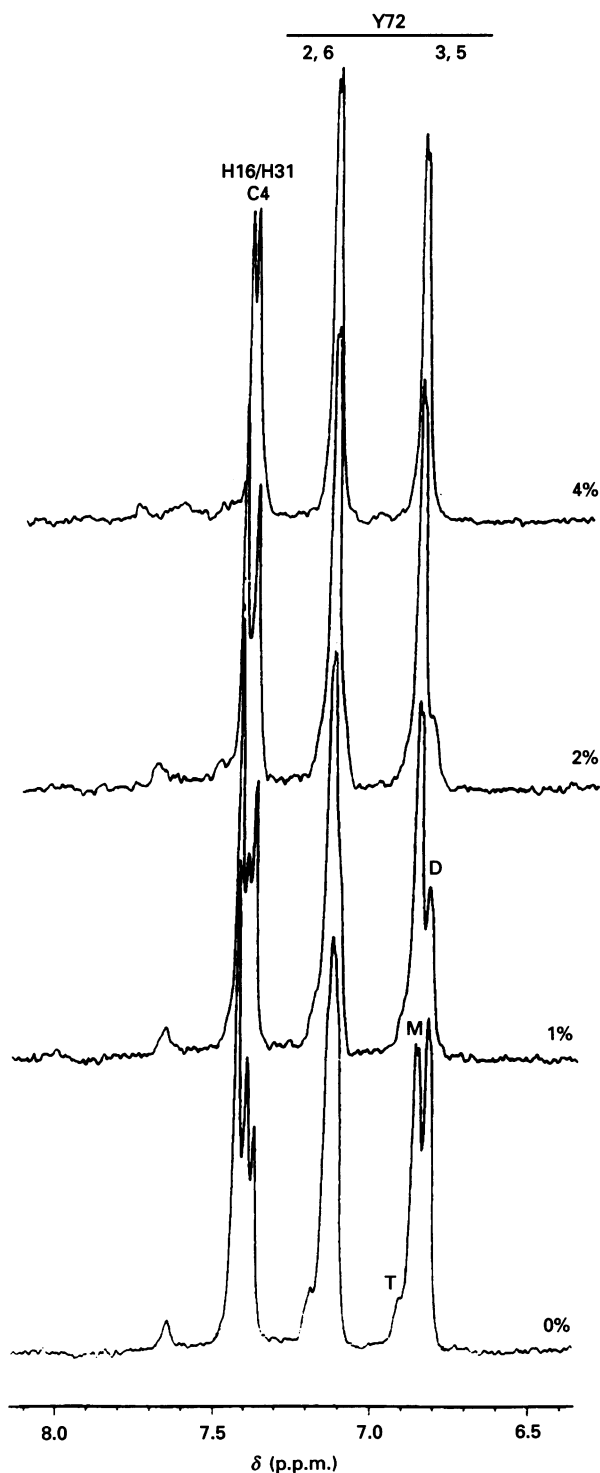


**Figure 1** Effect of 2-chloroethanol on NAP-2 aggregation

N.m.r. spectra of the aromatic proton resonance region for NAP-2, pH 4.0, 30 °C, are displayed in the presence of increasing concentrations (in % v/v) of 2-chloroethanol. Protein concentration is 10 mg/ml. Tyrosine-72 (Y72) 3,5 proton resonances have been labelled for monomer (M), dimer (D), and tetramer (T) aggregate states. Small downfield resonances are due to the presence of long-lived backbone amide proton resonances.

#### N.m.r. spectroscopy

Samples for  $^1\text{H}$ -n.m.r. measurements had been lyophilized and redissolved in  $^1\text{H}_2\text{O}$  or  $^2\text{H}_2\text{O}$  immediately before the experiment.

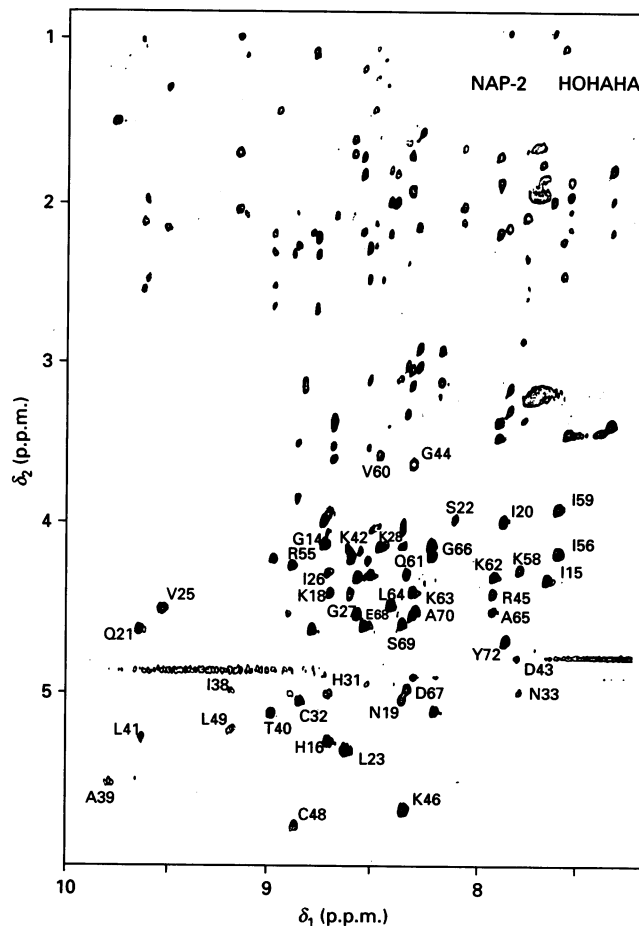


**Figure 2** HOHAHA spectrum of NAP-2

A two-dimensional-n.m.r. HOHAHA contour plot is shown for NAP-2 [pH 3.6, 4% (v/v) 2-chloroethanol, 40 °C]. The spin lock mixing time was 40 ms. Resonances and cross-peaks are labelled as described in the text. The single letter amino acid code is used.

For work in  $^1\text{H}_2\text{O}$  solutions, 10%  $^2\text{H}_2\text{O}$  was routinely used. The solution also contained 4% (v/v) perdeuterated 2-chloroethanol in order to dissociate dimer/tetramer aggregate states (Yang et al., 1993). The final protein concentration was 18 mg/ml. The pH was adjusted to pH 3.6 by adding microlitre increments of  $\text{NaO}^2\text{H}$  or  $^2\text{HCl}$  to 0.6 ml of sample. The pH was not adjusted for isotope effects.

$^1\text{H}$ -n.m.r. spectra were recorded in the Fourier mode on a Bruker AMX-600 spectrometer (600 MHz for protons). The  $^2\text{H}_2\text{O}$  deuterium signal was used as a field-frequency lock. All chemical shifts are quoted in parts per million (p.p.m.) downfield from sodium 4,4-dimethyl-4-silapentanesulphonate.

For sequential assignments, correlated spectroscopy (COSY) (Aue et al., 1976; Wider et al., 1984), double-quantum-filtered COSY (Piantini et al., 1982; Shaka and Freeman, 1983) and nuclear Overhauser effect spectroscopy (NOESY) (Jeener et al., 1979; Wider et al., 1984) experiments (mixing times of 0.05 s, 0.075 s, 0.1 s and 0.2 s) were performed. Two-dimensional-homonuclear Hartmann-Hahn magnetization transfer (HOHAHA) spectra, used to identify many spin systems completely, were obtained by spin-locking with an MLEV-17 sequence (Bax and Davis, 1985) with mixing times of 35 to 64 ms. All spectra were acquired in the phase-sensitive mode (States et al., 1982). The water resonance was suppressed by direct irradiation (1 s) at the water frequency during the relaxation

**Table 1** <sup>1</sup>H-n.m.r. sequence assignments (p.p.m.) for NAP-2Experimental conditions: pH 3.6, 313 K, 4% (v/v) 2-chloroethanol; H<sub>2</sub>O resonance 4.86 p.p.m. downfield from 4,4-dimethyl-4-silapentanesulphonate.

Residue	NH	$\alpha$ CH	$\beta$ CH <sub>2</sub>	others	Residue	NH	$\alpha$ CH	$\beta$ CH <sub>2</sub>	others
1. Met					37. Val	9.53	4.92	2.12	$\gamma$ H <sub>3</sub> 1.14
2. Ala	8.42	4.31	1.44		38. Ile	9.08	4.93	2.07	$\gamma$ H <sub>3</sub> 1.08
3. Glu	8.68	4.61	2.14, 2.25	$\gamma$ H <sub>2</sub> 2.58, 2.60					$\gamma$ H <sub>2</sub> 1.63, 1.97
4. Leu	8.46	4.53	1.76, 1.78	$\gamma$ H 1.70, 1.72					$\delta$ H <sub>3</sub> 1.02
				$\delta$ H <sub>3</sub> 0.97, 1.07	39. Ala	9.65	5.43	1.44	
5. Arg	8.23	4.79	1.94, 2.13	$\gamma$ H <sub>2</sub> 1.75, 1.77	40. Thr	8.87	5.07	4.23	$\gamma$ H <sub>3</sub> 1.38
				$\delta$ H <sub>2</sub> 3.37	41. Leu	9.51	5.2	2.38	$\gamma$ H 1.92
6. Cys	8.42	4.79	3.10, 3.50						$\delta$ H <sub>3</sub> 0.98
7. Met	8.80	4.97	2.25	$\gamma$ H <sub>2</sub> 2.72	42. Lys	8.51	4.18		
8. Cys	8.07	5.06	3.10, 3.24		43. Asp	7.67	4.77	2.38, 2.85	
9. Ile	8.48	4.76	2.12	$\gamma$ H <sub>3</sub> 1.06	44. Gly	8.18	3.73, 4.55		
				$\gamma$ H <sub>2</sub> 1.58, 1.86	45. Arg	7.8	4.42	2.19	$\gamma$ H <sub>2</sub> 1.88
				$\delta$ H <sub>3</sub> 0.96					$\delta$ H <sub>2</sub> 3.38
10. Lys	(H <sup>2</sup> O)	4.82	1.65	$\gamma$ H <sub>2</sub> 1.94	46. Lys	8.22	5.70	1.69	$\gamma$ H <sub>2</sub> 1.79
				$\delta$ H <sub>2</sub> 2.07					$\gamma$ H <sub>2</sub> 1.89
				$\epsilon$ H <sub>2</sub> 3.22					$\delta$ H <sub>2</sub> 3.15
11. Thr	8.4	4.91	4.26	$\gamma$ H <sub>3</sub> 1.4	47. Ile	9.03	4.95	2.01	$\gamma$ H <sub>3</sub> 1.03
12. Thr	8.36	4.83	4.03	$\gamma$ H <sub>3</sub> 1.42					$\gamma$ H <sub>2</sub> 1.33
13. Ser	8.61	4.81	4.15, 4.12						$\delta$ H <sub>3</sub> 0.96
14. Gly	8.63	4.04, 4.17			48. Cys	8.76	5.78	3.47, 3.93	
15. Ile	7.53	4.35	1.95	$\gamma$ H <sub>3</sub> 1.03	49. Leu	9.06	5.16	1.62, 1.97	$\gamma$ H 1.31
				$\gamma$ H <sub>2</sub> 1.47, 1.82					$\delta$ H <sub>3</sub> 0.94
				$\delta$ H <sub>3</sub> 0.93	50. Asp	8.25	4.58	2.8, 3.06	
16. His	8.59	5.22	3.35, 3.48	1H 8.76	51. Pro	—	4.10	1.94, 2.16	$\gamma$ H <sub>2</sub> 1.97
				2H 7.42					$\delta$ H <sub>2</sub> 4.13, 4.47
17. Pro	—	4.33	2.04, 2.31	$\gamma$ H <sub>2</sub> 2.11	52. Asp	8.07	4.33	2.91, 3.10	
				$\delta$ H <sub>2</sub> 4.05, 4.09	53. Ala	7.59	4.73	1.73	
18. Lys	8.60	4.42			54. Pro	—	4.52	2.01, 2.25	$\gamma$ H <sub>2</sub> 2.03
19. Asn	8.23	5.0	3.01, 3.28						$\delta$ H <sub>2</sub> 4.04, 4.20
20. Ile	7.75	4.04	2.18	$\gamma$ H <sub>3</sub> 1.1	55. Arg	8.78	4.28	2.01, 2.11	$\gamma$ H <sub>2</sub> 1.83, 1.92
				$\gamma$ H <sub>2</sub> 1.56					$\delta$ H <sub>2</sub> 3.42
				$\delta$ H <sub>3</sub> 0.94	56. Ile	7.47	4.2	2.41	$\gamma$ H <sub>3</sub> 1.04
				$\gamma$ H <sub>2</sub> 2.45, 2.61					$\gamma$ H <sub>2</sub> 1.69
21. Gln	9.52	4.62	2.04, 2.18						$\delta$ H <sub>3</sub> 0.94
22. Ser	7.98	4.73	4.03						
23. Leu	8.51	5.27	1.67	$\gamma$ H 1.60	57. Lys	8.44	4.2		
				$\delta$ H <sub>3</sub> 0.96	58. Lys	7.66	4.29		
24. Glu	8.88	4.91	2.15, 2.26	$\gamma$ H <sub>2</sub> 2.45, 2.59	59. Ile	7.48	3.97	2.12	$\gamma$ H <sub>3</sub> 1.06
25. Val	9.41	4.50	2.08	$\gamma$ H <sub>3</sub> 1.23					$\gamma$ H <sub>2</sub> 1.58
26. Ile	8.61	4.31	2.13	$\gamma$ H <sub>3</sub> 1.03					$\delta$ H <sub>3</sub> 0.95
				$\gamma$ H <sub>2</sub> 1.67	60. Val	8.36	3.68	2.44	$\gamma$ H <sub>3</sub> 1.11, 1.18
				$\delta$ H <sub>3</sub> 0.91	61. Gln	8.23	4.17	2.03, 2.09	$\gamma$ H <sub>2</sub> 2.26
27. Gly	8.49	4.23, 4.42			62. Lys	7.79	4.33		
28. Lys	8.34	4.17	1.64, 1.73	$\gamma$ H <sub>2</sub> 1.41	63. Lys	8.18	4.42		
				$\delta$ H <sub>2</sub> 1.63	64. Leu	8.29	4.485	1.95	$\gamma$ H 1.77
				$\epsilon$ H <sub>2</sub> 3.15					$\delta$ H <sub>3</sub> 1.05
29. Gly	8.61	4.0, 4.34			65. Ala	7.80	4.52	1.67	
30. Thr	8.22	4.79	4.52	$\gamma$ H <sub>3</sub> 1.3	66. Gly	8.09	4.15, 4.22		
31. His	8.59	4.96	3.3, 3.56	1H 8.67	67. Asp	8.17	4.94	3.03, 3.12	
				2H 7.44	68. Glu	8.43	4.60	2.27	$\gamma$ H <sub>2</sub> 2.75, 2.81
32. Cys	8.74	5.01	3.07, 3.13		69. Ser	8.18	4.87	4.05, 4.09	
33. Asn	7.65	4.94	3.0, 3.36		70. Ala	8.16	4.53	1.55	
34. Gln	8.39	4.25	2.09, 2.21	$\gamma$ H <sub>2</sub> 2.52, 2.58	71. Asp	7.84	4.81		
35. Val	8.22	4.32	2.21	$\gamma$ H <sub>3</sub> 1.22	72. Tyr	7.73	4.68	3.14, 3.27	$\delta$ H <sub>2</sub> 7.12
36. Glu	8.54	4.78							$\epsilon$ H <sub>2</sub> 6.85

delay between scans as well as during the mixing time in NOESY experiments.

The majority of two-dimensional-n.m.r. spectra were collected as 512 or 1024  $t_1$  experiments, each with 1 k or 2 k complex data points over a spectral width of 6 kHz in both dimensions with the carrier placed on the water resonance. 64 or 96 scans were generally time-averaged per  $t_1$  experiment. The data were processed directly on the Bruker AMX-600 X-32 or off-line on a Sun SPARC-II computer workstation with Bruker UXMNRP or

FELIX programs. Data sets were multiplied in both dimensions by 0 to 60°-shifted sine-bell or lorentzian to gaussian transformation functions and generally zero-filled to 1 k in the  $t_1$  dimension before Fourier transformation.

For identification of long-lived backbone amide protons, HOHAHA (Aue et al., 1976; Wider et al., 1984) experiments were performed at 5 °C and pH 3.6. Peptide was first exchanged and freeze-dried from <sup>1</sup>H<sub>2</sub>O solution. <sup>2</sup>H<sub>2</sub>O at ice bath temperature was then added to the dried peptide kept in the n.m.r.

tube on ice. A HOHAHA experiment was run for approx. 3 h, collecting 256 time-incremented 1 k data point free induction decays (FIDs), each with 32 transients. Data sets were first multiplied in both dimensions by a 30°-shifted, sine-squared bell function and zero-filled to 512 in the  $t_1$  dimension before Fourier transformation. Long-lived backbone amide protons were identified by comparing cross-peak positions to sequentially assigned HOHAHA data sets accumulated under the same conditions, but in the presence of mostly  $^1\text{H}_2\text{O}$  (90%  $^1\text{H}_2\text{O}/10\%$   $^2\text{H}_2\text{O}$ ) where NH resonances were present.  $\alpha\text{N}$  cross-peaks which remained during the  $^2\text{H}_2\text{O}$  HOHAHA accumulation are called 'long-lived' in the paper, i.e. the larger the cross-peak, the longer the relative life time.

## RESULTS AND DISCUSSION

Like PF4 (Mayo and Chen, 1989) and LA-PF4 (Mayo, 1991), NAP-2 gives  $^1\text{H}$ -n.m.r. spectra (600 MHz) which show the presence of slow exchange (n.m.r. chemical-shift time scale) among monomer-dimer-tetramer aggregate states (Figure 1). This not only complicates n.m.r. conformation analysis, but causes severe problems arising from chemical exchange. Since relatively low concentrations of 2-chloroethanol are known to disrupt PF4 subunit association by shifting monomer-dimer-tetramer equilibria to lower aggregate states and by increasing subunit exchange rates (Yang et al., 1993), NAP-2 solutions titrated with 2-chloroethanol were found to be predominantly in

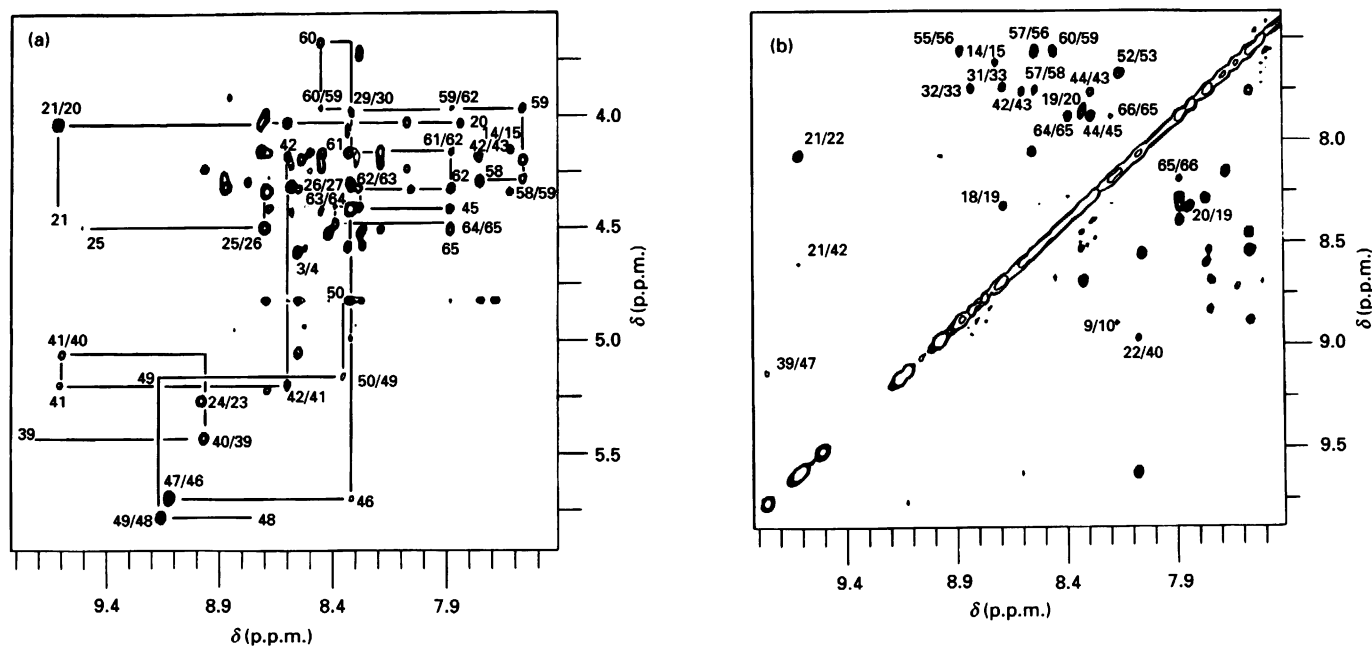


**Figure 3** NOESY  $\alpha\text{N}$  fingerprint and NH-NH regions of NAP-2

The  $\alpha\text{CH}$ -NH fingerprint (a) and NH-NH (b) resonance regions from a NOESY contour plot are shown for NAP-2, pH 3.6, 4% (v/v) 2-chloroethanol, 40 °C. Data were collected in 90%  $^1\text{H}_2\text{O}/10\%$   $^2\text{H}_2\text{O}$  (before the addition of the 4% 2-chloroethanol). Protein concentration was 18 mg/ml. 512 hypercomplex FIDs containing 1 k words were collected and processed as discussed in the Materials and methods section. The mixing time was 0.075 s. The data were zero-filled to 1024 in  $t_1$ . The raw data were then multiplied by a 30°-shifted sine-squared function in  $t_1$  and  $t_2$  prior to Fourier transformation. Some sequential resonance assignments are traced out, and some longer-range nOes are indicated. Labelling of resonances is as discussed in the text.



**Figure 4** Summary of n.m.r./nOe data for NAP-2

The NAP-2 protein sequence is shown with a summary of identifiable nOes for data accumulated at pH 3.6, 4% (v/v) 2-chloroethanol, at 30 °C and 40 °C. nOes are tabulated in the format discussed by Wüthrich (1986).  $^3J_{\alpha\text{N}}$  coupling constants for some residues are indicated with a filled-in square for those greater than 8 Hz and with a filled-in circle for those less than 6 Hz. Long-lived backbone NHs are indicated with a filled-in square.

the monomer state (more than 95%) by addition of 3–4% (v/v) 2-chloroethanol (see Figure 1). For n.m.r. structural analysis of NAP-2 therefore the best solution conditions were at pH values about pH 3.6, with 4% (v/v) 2-chloroethanol at temperatures between 30 °C and 50 °C. It should be noted that unlike PF4, which exists in solution in a probably functional tetramer state under physiological conditions, NAP-2 exists mostly in the monomer state at physiological pH and ionic strength (Mayo, 1991) given its normal concentration in the serum of clotted blood, i.e. 5–35 µg/ml (Castor et al., 1990). In this respect, study of the NAP-2 monomer state is most relevant. To date, tetrameric PF4 (St. Charles et al., 1989; Zhang et al., 1993) and dimeric IL-8 (Clore et al., 1989) have been structurally investigated. This present study, therefore, provides an added dimension by addressing NAP-2 monomer folding in the absence of conformational stabilizing/modifying subunit associations.

Sequence-specific proton resonance assignments were performed by using established procedures (Wüthrich, 1986). Spin systems were initially identified by analysing HOHAHA and COSY spectra and then sequentially assigned using NOESY spectra. Various ambiguities arising from chemical-shift degeneracies were mostly resolved by recording spectra at different temperatures from 30 °C to 50 °C. A typical HOHAHA contour plot is shown in Figure 2 with many sequential assignments labelled. Due to the presence of crowded regions and overlap of some  $\alpha$ H resonances with the  $H^2HO$  resonance, not all HOHAHA  $\alpha$ N cross-peaks have been labelled. A more complete list of sequence-specific resonance assignments is given in Table 1.

NOESY spectra are exemplified in Figure 3 which shows the  $\alpha$ N fingerprint and NH-NH regions. Some sequential connectivities are traced out, and a few longer-range nuclear Overhauser effects (nOes) are indicated in the Figure. The NH-NH region indicates a continuous series of NH connectivities in the C-terminal domain.

Elements of secondary structure can be deduced from a qualitative interpretation of nOe,  $^3J_{\alpha N}$  coupling constants and long-lived backbone NHs presented in Figure 4. Anti-parallel  $\beta$ -sheet alignments consistent with these data are indicated in Figure 5. Double-sided arrows indicate observed nOe connectivities. Broken lines suggest hydrogen bonds consistent with these structural elements and with observed long-lived NHs.

Given the fact that NAP-2 contains only one tyrosine and two histidines, few side-chain to side-chain nOes could be identified. It is these nOes which best define overall folding, in particular how the C-terminal helix is positioned on top of the anti-parallel  $\beta$ -sheet domain. However, in instances of more localized conformation where inter-residue backbone constraints are sufficient to define structure, i.e. helix and  $\beta$ -sheet, folding patterns may be determined. For NAP-2, therefore, this study is limited to the derivation of secondary structural elements and folding within the  $\beta$ -sheet domain.

NAP-2 contains a triple-stranded anti-parallel  $\beta$ -sheet arranged in a 'Greek key' with strand 2 (residues 35–41) hydrogen-bonded to strands 1 (residues 22–27/28) and 3 (residues 45–50). Strands 1 and 2 are connected by a loop (residues 29/30–34) which shows elements of a turn centred at residues 31–32. This turn is folded proximal to the N-terminus tripeptide sequence ELR which appears to be associated with neutrophil activation. Strands 2 and 3 are connected by a 3:5-hairpin (residues 42–45) comprising a  $\beta$ -turn and G1  $\beta$ -bulge (Sibanda and Thornton, 1985). As shown by strong  $H_{(i,i-1)}-H_i$  nOes, all three proline residues, Pro-17, Pro-51 and Pro-54, have their peptide bonds in the *trans* conformation. Apparent turns are also centred around residues 6–7, 9–10, 13–14, and 51–52. A helix-

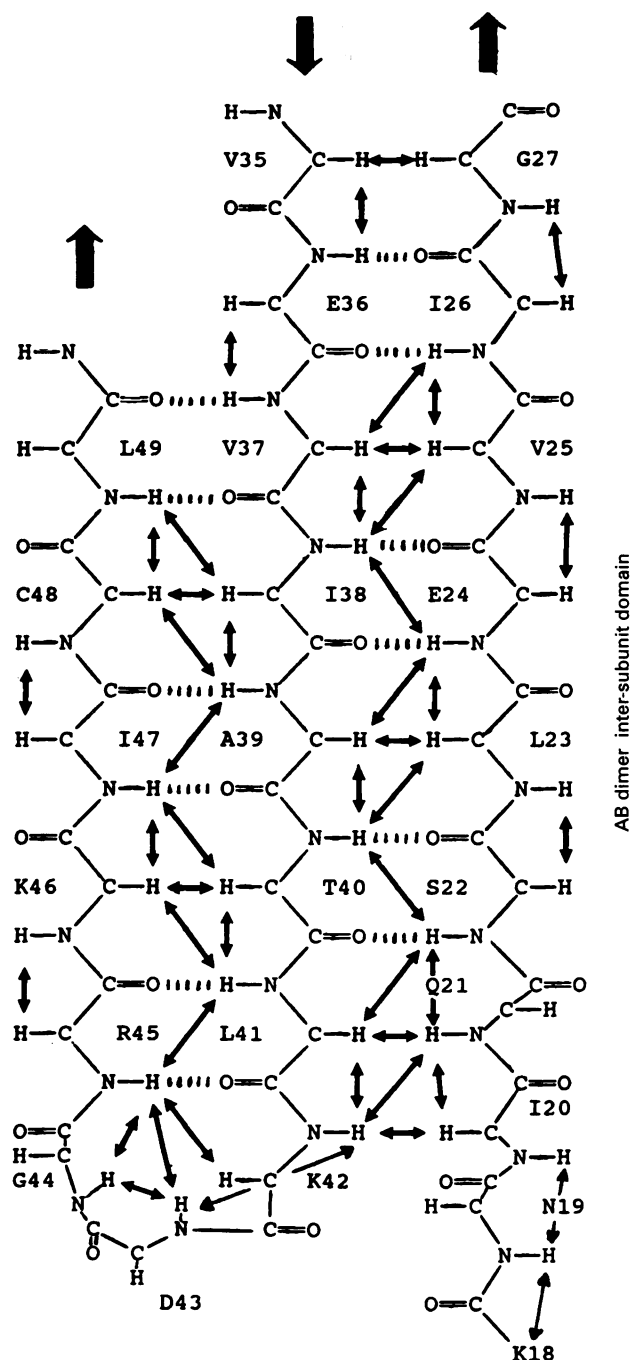


Figure 5 Anti-parallel  $\beta$ -sheet in NAP-2

A schematic representation showing backbone folds in NAP-2 is given. This structure is consistent with n.m.r. data as described in the text. Double-sided arrows indicate observed nOes and broken lines suggest NH hydrogen bonds proposed on the basis of long-lived NHs and this folding pattern. Residue numbering is as given in Figure 3 and in Table 1.

like turn within residues 18–21 leads into  $\beta$ -sheet strand 1. Residues 55–67 form a C-terminal helix. The last five C-terminal residues are structurally less descriptive due to the lack of n.m.r./nOe information.

Among PF4, IL-8 and NAP-2, the length of the C-terminal  $\alpha$ -helix varies. In PF4 and NAP-2, the C-terminal helix runs 11 and 13 residues respectively, while in IL-8 it runs 18 residues. In NAP-2, the helix runs from Arg-55 to Asp-67. For IL-8 (Clore

et al. 1989) and PF4 (Zhang et al., 1993), this helix extends up to the final C-terminal serine residue, while for NAP-2 Gly-66 and Asp-67 give considerably weaker inter-residue helix nOes, and the paucity of nOes within the last five potential helical residues suggests significant internal mobility of the NAP-2 C-terminus in the monomeric state. In tetrameric PF4 (Zhang et al., 1993) and dimeric IL-8 (Clore et al., 1989), the final C-terminal serine in one subunit is anchored via inter-residue electrostatic interactions with an opposing subunit. This suggests that subunit associations stabilize the C-terminal conformation from about the helix glycine C-cap position (Richardson and Richardson, 1988).

In terms of the role of the C-terminus in heparin binding, this study verifies the existence of the NAP-2 (LA-PF4) C-terminal helix. It has been proposed (Lawler, 1981; Cowan et al., 1986) that part of the reduced NAP-2 (LA-PF4) heparin binding relative to that in PF4 may be due to the spatial mis-alignment of the four C-terminal lysine residues when in a helix conformation. The fourth lysine residue in NAP-2 is folded more towards the hydrophobic face of the amphipathic helix, where it may form a salt-bridge with Asp-67 or Glu-68. Recent results with PF4 C-terminal lysine-to-alanine variants (Mayo, Barker, Ilyina, Daly and La Rosa, unpublished work) show that removal of any one of the four C-terminal lysines, however, does not significantly affect heparin binding in PF4. This suggests that non-C-terminal amino acid residues are also important to heparin binding; and that the NAP-2 sequential mis-alignment probably has less to do with heparin binding than originally thought. Furthermore, the ring of positively-charged amino acids identified about tetrameric PF4 probably would exist in tetrameric NAP-2 based on the present structural information. This ring includes the C-terminal lysines, as well as His-16, Lys-18, Lys-42, Arg-45 and Arg-55. Attenuated subunit association in NAP-2 remains the most viable explanation for reduced heparin affinity in NAP-2 (Mayo, 1991).

This work was supported by a grant from the National Heart, Lung and Blood Institute (HL-43194) and by Repligen Corporation.

## REFERENCES

- Anisowicz, A., Bardwell, L. and Sager, R. (1987) *Proc. Natl. Acad. Sci. U.S.A.* **84**, 7188–7192
- Aue, W. P., Bartholdi, E. and Ernst, R. R. (1976) *J. Chem. Phys.* **64**, 2229–2246
- Bax, A. and Davis, D. G. (1985) *J. Magn. Reson.* **65**, 355–360
- Begg, G. S., Pepper, D. S., Chesterman, C. N. and Morgan, F. J. (1978) *Biochemistry* **17**, 1739–1744
- Bidlingmeyer, B. A., Cohen, S. A. and Tarvin, T. L. (1984) *J. Chromatogr.* **336**, 93–100
- Castor, C. W., Miller, J. W. and Walz, D. A. (1983) *Proc. Natl. Acad. Sci. U.S.A.* **80**, 765–769
- Castor, C. W., Walz, D. A., Johnson, P. H., Hossler, P. A., Smith, E. M., Bignall, M. C., Aaron, B. P., Underhill, P., Lazar, J. M., Hudson, D. H., et al. (1990) *J. Lab. Clin. Med.* **116**, 516–526
- Clore, G. M., Appella, E., Yamada, M., Matsushima, K. and Gronenbron, A. M. (1989) *Biochemistry* **29**, 1689–1696
- Cowan, S., Bakshi, E. N., Machin, K. J. and Issacs, N. W. (1986) *Biochem. J.* **234**, 485–488
- Deuel, T. F., Keim, P. S., Farmer, M. and Heinrichson, R. L. (1977) *Proc. Natl. Acad. Sci. U.S.A.* **74**, 2256–2258
- Holt, J. C., Harris, M. E., Holt, A., Lange, E., Henschen, A. and Niewiarowski, S. (1986) *Biochemistry* **25**, 1988–1996
- Holt, J. C., Yan, Z. O., Lu, W. Q., Stewart, G. J. and Niewiarowski, S. (1992) *Proc. Soc. Exp. Biol. Med.* **199**, 171–177
- Jeener, J., Meier, B., Backman, P. and Ernst, R. R. (1979) *J. Chem. Phys.* **71**, 4546–4550
- Lawler, J. W. (1981) *Thromb. Res.* **21**, 121–127
- Lowry, O. H., Rosbough, N. J., Fan, A. L. and Randall, R. J. (1951) *J. Biol. Chem.* **193**, 265–270
- Mayo, K. H. (1991) *Biochemistry* **30**, 925–934
- Mayo, K. H. and Chen, M. J. (1989) *Biochemistry* **28**, 9469–9478
- Miller, M. D. and Krangel, M. S. (1992) *Crit. Rev. Immunol.* **12**, 17–46
- Moser, B., Schumacher, C., von Tscharnar, V., Clark-Lewis, I. and Baggiolini, M. (1991) *J. Biol. Chem.* **266**, 10666–10671
- Myers, J. A., Gray, G. G., Peters, D. J., Grimaila, R. J., Hunt, A. J., Maione, T. E. and Mueller, W. T. (1991) *Protein Expression Purification* **2**, 136–143
- Piantini, U., Sørensen, O. W. and Ernst, R. R. (1982) *J. Am. Chem. Soc.* **104**, 6800–6805
- Rajaraman, K., Sykes, B. D., Kay, C. M., Dewald, B., Geiser, T., Baggiolini, M. and Clark-Lewis, I. (1994) *Science* **264**, 90–92
- Richardson, J. S. and Richardson, D. C. (1988) *Science* **240**, 1648–1652
- Schmid, J. and Weissmann, C. (1987) *J. Immunol.* **139**, 250–256
- Schnitzel, W., Garbeis, B., Monschein, U. and Besemer, J. (1991) *Biochem. Biophys. Res. Commun.* **18**, 301–307
- Schumacher, C., Clark-Lewis, I., Baggiolini, M. and Moser, B. (1992) *Proc. Natl. Acad. Sci. U.S.A.* **89**, 10542–10546
- Shaka, A. J. and Freeman, R. (1983) *J. Magn. Reson.* **51**, 161–169
- Sibanda, B. L. and Thornton, J. M. (1985) *Nature (London)* **316**, 170–174
- Smith, P. K., Krohn, R. I., Hermanson, G. T., Mallia, A. K., Gartner, F. H., Provenzano, M. D., Fujimoto, E. K., Goeke, N. M., Olson, B. J. and Klenk, D. C. (1985) *Anal. Biochem.* **150**, 76–85
- St. Charles, R., Walz, D. A. and Edwards, B. F. P. (1989) *J. Biol. Chem.* **264**, 2092–2099
- States, D. J., Haberkorn, R. A. and Ruben, D. J. (1982) *J. Magn. Reson.* **48**, 286–293
- Van Osselaer, N., Van Damme, J., Rampart, M. and Herman, A. G. (1991) *Am. J. Pathol.* **138**, 23–27
- Waddell, W. J. (1956) *J. Lab. Clin. Med.* **48**, 311–314
- Walz, A., Dewald, B., von Tscharnar, V. and Baggiolini, M. (1989) *J. Exp. Med.* **170**, 1745–1750
- Wider, G., Macura, S., Anil-Kumar, Ernst, R. R. and Wüthrich, K. (1984) *J. Magn. Reson.* **56**, 207–234
- Wüthrich, K. (1986) *N.m.r. of Proteins and Nucleic Acids*, Wiley-Interscience, NY
- Yang, Y., Barker, S., Chen, M.-J. and Mayo, K. H. (1993) *J. Biol. Chem.* **268**, 9223–9229
- Zhang, X., Chen, L. and Bancroft, D. P. (1994) *Biochemistry* **33**, 8361–8366